Photoacoustics 12 (2018) 6–13

Contents lists available at ScienceDirect

Photoacoustics

journal homepage: www.elsevier.com/locate/pacs

Research article

Adjustable photoacoustic tomography probe improves light delivery and image quality

Gurneet S. Sangha[a], Nicholas J. Hale[a], Craig J. Goergen[a,b,*]

[a] Weldon School of Biomedical Engineering, Purdue University, 206 S. Martin Jischke Dr., West Lafayette, IN 47907, USA
[b] Purdue University Center for Cancer Research, Purdue University, 201 S. University St., West Lafayette, IN 47907, USA

ARTICLE INFO

Keywords:
Photoacoustic
Ultrasound
Monte Carlo
Artifact
Signal-to-noise
Imaging

ABSTRACT

One cause for suboptimal photoacoustic tomography (PAT) penetration depth is attenuation of incident light by soft tissue. To better understand this problem, we investigated the effects of illumination fiber optic bundle geometry on PAT penetration depth and signal-to-noise ratio. An adjustable, motorized PAT probe was used to reduce probe-skin reflection artifacts and improve light distribution in the image acquisition plane by tuning fiber orientation. We validated our motorized PAT probe through Monte Carlo simulations and *ex vivo* imaging of a tissue mimicking phantom, and *in vivo* imaging of murine periaortic fat. Overall, our *ex vivo* results showed a several millimeter improvement in penetration depth and *in vivo* results showed a > 62% increase in lipid signal-to-noise ratio. Our PAT probe also utilized a 7-μm aluminum filter to block *in vivo* probe-skin reflection artifacts. Together, these findings showed the importance of optimizing illumination geometry to enhance PAT image quality.

1. Introduction

Photoacoustic Tomography (PAT) has been shown to provide real-time compositional information of tissue without the need for exogenous contrast agents and with superior penetration depth compared to conventional optical techniques [1–3]. These optical barriers are overcome since PAT does not rely on conventional ballistic photons, but rather detects acoustic waves that are thermoelastically produced by photon-tissue interactions [1–3]. Therefore, PAT can provided useful compositional information that complements current clinical imaging modalities, thus emphasizing the capability of this imaging approach to improve medical care. These characteristics highlight the potential of the technology to be used for a variety of biomedical applications including atherosclerosis [4–9], cancer [10–12], and nerve imaging [13].

While PAT has shown great potential, there are still certain biological barriers that have limited its use. For example, applications for high-resolution noninvasive lipid-based imaging are limited to roughly 3 mm due to subcutaneous fat absorbers, as well as the intrinsic light attenuation due to optical properties of tissue [4,14]. Therefore, there is still a need for further PAT optimization to fully utilize its capabilities. Previous works have utilized image processing and instrumentation engineering to improve image quality and eliminate PAT-specific artifacts. Light catching mechanisms have been particularly useful for redirecting reflected light back into tissue to increase photon density, thus improving signal intensity [15–17]. While effective, the combination of this approach and manually tuning the angle of the fiber optic bundles to improve photon density at various depths may be a superior technique for improving image quality. This is further supported by previous works that have shown that tissue light distribution is effected by illumination geometry [18,19]. Therefore, we hypothesized that by manipulating fiber-ultrasound orientation we can optimize light penetration into tissue, thus improving penetration depth and signal-to-noise ratio (SNR). Light tuning is dependent on fundamental photoacoustic principles where an initial photoacoustic pressure rise (p_o) results from light-induced thermoelastic expansion as characterized by Eq. (1).

$$p_o = \Gamma \mu_a F \tag{1}$$

Here the pressure rise p_o is dependent upon the Grüneisen parameter (Γ), absorption coefficient (μ_a), and optical fluence (F) if we assume that all of the absorbed light is converted to heat energy [1,20]. The Grüneisen parameter is further defined by Eq. (2), where α is the isobaric volume thermal expansion coefficient, κ is the isothermal compressibility, ρ is the density of the sample, and C_p is the specific-heat capacity.

$$\Gamma = \alpha / (\kappa \rho C_p) \tag{2}$$

These parameters, including μ_a, are dependent on the innate tissue

* Corresponding author at: Weldon School of Biomedical Engineering, Purdue University, 206 S. Martin Jischke Dr., West Lafayette, IN 47907, USA.
E-mail address: cgoergen@purdue.edu (C.J. Goergen).

https://doi.org/10.1016/j.pacs.2018.08.002
Received 19 April 2018; Received in revised form 20 July 2018; Accepted 9 August 2018
Available online 22 August 2018

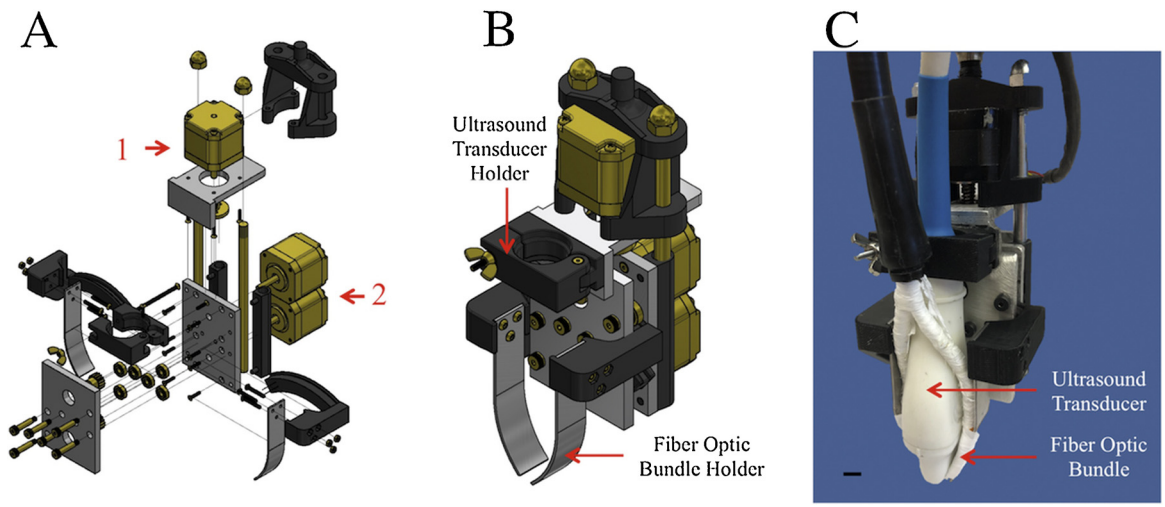

Fig. 1. Exploded (A), presentation (B), and constructed (C) images of the PAT holder. Fabricated parts shown in silver, 3D printed parts shown in black, and commercially available parts shown in gold. PAT holder specifically consists of motors for translation of ultrasound transducer (1), and rotation of fiber optic bundles (2). Scale bar represents 1 cm.

properties; therefore we can assume that increasing photon density in the tissue can increase the PAT signal amplitude. Taken together, we aim to design tunable fiber optic PAT probes that can enhance image quality for a wide variety of applications.

Digital image processing techniques have played a tremendous role in minimizing in-plane artifacts and out-of-plane clutter [21,22], however, in some cases artifact prevention strategies may be a more appropriate solution to improve image quality. PAT reflection artifacts is one such example where light reflects off of the skin surface that causes a photoacoustic (PA) effect at the probe face rather than within the sample [23]. This PA ultrasound wave then travels and reflects off of the skin surface, registering in the ultrasound system as originating at a distance two times the probe to skin spacing (Fig. 5A). Singh et al. has previously developed a simple yet effective PAFUSion technique to remove PAT reflection artifacts without the need of additional transducers or algorithms [24,25]. This approach uses the ultrasound transducer to acquire two images where one image is focused on the optical absorber and the other is focused on the acoustic reflector induced artifact. A weighted addition is then performed and used to recreate a corrected image without the reflection artifact. While this approach is effective, we explore an alternative solution by which an aluminum filter is used to decouple the optical absorbance by the ultrasound transducer to eliminate the reflection artifact. We quantitatively evaluate the use of a light reflecting material over our PA probe to prevent optical absorption by the transducer and adequately remove this probe-skin interaction artifact.

Here, we propose to use a method whereby the fiber optic bundles are tuned to increase photon density in the image acquisition plane. This method can be coupled with other light manipulation techniques, such as the light catching mechanism, to further improve penetration depth and SNR. We introduce our methods to design and build a PAT holder that allows tuning of the fiber optic bundle orientation. We also investigate the effect of fiber optic bundle orientation on tissue light distribution using Monte Carlo multilayer (MCML) modeling. We then compared these results to *ex vivo* and *in vivo* studies were we used focal length to quantify changes in image quality, as we believe this is a more intuitive experimental metric compared to fiber optic bundle angle. We defined focal length as the distance between the bifurcated fiber optic bundles and where the two incident light beams converge. This should not be confused with the transducer focus, which is defined as the depth with the narrowest acoustic beam width. We also present a straightforward and effective method to remove reflection artifacts that can be used on virtually all PAT imaging systems. Overall, the work described here suggests that PAT illumination geometry should be optimized for different biological tissues due to varying optical tissue heterogeneity and to minimize in-plane artifacts and out-of-plane clutter.

2. Methods

2.1. Photoacoustic system design

The PAT system utilized in this study consists of a high-frequency small animal ultrasound system (Vevo2100, FUJIFILM Visual Sonics) and an Nd:YAG pulsed optical parametric oscillator (OPO) laser (Surelite EX, Continuum). Ultrasound system was equipped with a 40 MHz center frequency transducer (MS550D) that allowed the user to acquire images with an axial resolution of 40 μm. The Nd:YAG laser was capable of producing 5 ns pulses at 10 Hz ranging from 670 to 2500 nm. Pulsed light was delivered from the laser to the sample through a 2 m fiber optic bundle with a opening diameter of 1.0 cm and rectangular terminals of 18 mm × 2 mm. This allowed us to produce an optical fluence of 40 mJ/cm^2, which is below the American National Standards Institute (ANSI) safety standards [26]. A pulse generator (9200, Quantum Composers) synchronized laser excitation with ultrasound and PAT image acquisition by sending 1) appropriately timed 10 Hz, 5 V inverted signals to the laser q-switch and flash lamp and 2) a normal 10 Hz, 5 V pulse signal to the ultrasound system. Finally, to prevent acoustic focus induced changes in SNR the transducer focus was set to 7 mm for *ex vivo* validation imaging and 5 mm for *in vivo* validation imaging.

2.2. Photoacoustic tomography fiber-adjusting apparatus design

The PAT fiber-tuning apparatus was first designed using Autodesk Inventor Professional Student Edition (Fig. 1A and B) and built using both 3D printed and fabricated 6061-T6 aluminum parts, as well as commercially available hardware (Fig. 1C). The 3D printed parts were printed from Acrylonitrile Butadiene Styrene plastic using a Stratasys Fortus 400mc 3D Production System. The arms that hold fiber cables were made of 16-gauge-carbon steel, while the remaining plates that mount the stepper motors are made from 0.25 in. 6061-T6 aluminum. A 12 V Nema 17 external linear stepper motor (17LS13-0404E-100H, StepperOnline), a 5.4 V Nema 17 bipolar stepper motor (17HM15-0904S, StepperOnline), and a Stepoko 3-axis controller (ROB-13899, SparkFun) were used to adjust the translation of the ultrasound transducer and rotation of the fiber optic bundles. The external linear